Applied Mathematics and Computation 433 (2022) 127368

Contents lists available at ScienceDirect

Applied Mathematics and Computation

journal homepage: www.elsevier.com/locate/amc

Prey–predator dynamics with adaptive protection mutualism

Tomás A. Revilla[a,b,*], Vlastimil Křivan[a,b]

[a] Czech Academy of Sciences, Biology Centre, Institute of Entomology, Branišovská 31, České Budějovice 370 05, Czech Republic
[b] Department of Mathematics, Faculty of Science, University of South Bohemia, Branišovská 1760, České Budějovice 370 05, Czech Republic

ARTICLE INFO

Article history:
Received 19 August 2021
Revised 9 May 2022
Accepted 27 June 2022

Keywords:
Predation
Defensive mutualism
Optimal foraging
Ants
Piecewise-smooth systems

ABSTRACT

Prey can ease the burden of exploitation by attracting a third party that interferes with their predators. Such is the case for plant-ant or aphid-ant mutualisms , where the victim supplies food to the ants, while the ants attack or drive away the offenders. Since ants are adaptive foragers, defense services can be altered by alternative food sources (e.g., other plants, or human-supplied resource). This article explores the prey-predator-ant system, using a model that combines predator-prey population dynamics with ant optimal foraging, where ants consume prey-supplied resources or alternative resources. Feedbacks between prey-predator dynamics and adaptive ant foraging leads to complex dynamics. For a given ant colony size and supply rate of alternative resources, prey can coexist with predators at alternative stable states, or along alternative limit cycles. Limit cycles extend the scope of defensive mutualism beyond the point where ants would abandon prey in favor of alternative resources under equilibrium conditions. These results highlight the importance of trait-mediated indirect interactions for natural mutualistic–antagonistic systems, and potential outcomes of manipulating ant defense services using baits in the case of agriculture.

1. Introduction

Many resource-consumer trophic interactions are influenced by a third, modifier species [e.g., 14] that changes the prey-predator interaction strength. E.g., an alternative prey can weaken the focal prey-predator interaction strength when the focal prey density is low and the predator switches to the alternative prey which can lead to the focal prey-predator coexistence that would be otherwise impossible [e.g., 1, [3,22,25], 46]. One important modifier is protection mutualism where a prey mutualist weakens interaction strength between the prey and its predator. An important case of protection mutualism occurs in systems with ants.

Ants are a highly diverse insect group (Hymenoptera, Formicidae) that maintains mutualisms with all sorts of plants, animals and fungi. They organize as colonies of genetically related individuals with a complex division of labor. Activities such as scouting, foraging, nursing of immatures, building structures, attack and defense, can be very adaptable to current demands of energy and resources. As a result of this flexibility, and owing to their large numbers, ants have large impacts, both antagonistic and mutualistic, on the populations with which they interact [7].

* Corresponding author at: Czech Academy of Sciences, Biology Centre, Institute of Entomology, Branišovská 31, České Budějovice 370 05, Czech Republic.
E-mail address: tomrevilla@gmail.com (T.A. Revilla).

https://doi.org/10.1016/j.amc.2022.127368

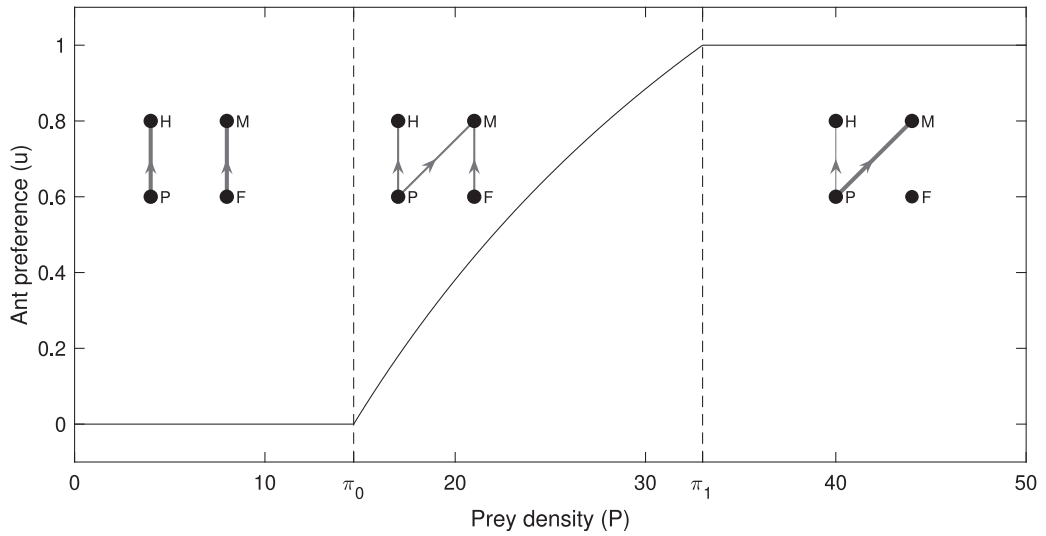

Fig. 1. Adaptive ant foraging preference for the prey-supplied resource (4) as a function of prey density. If $P \le \pi_0$ given in (5a), ants (M) forage exclusively on alternative resources (F), and do not interfere with predators (H). Increased preference for prey-supplied resources for prey densities between $\pi_0 = 14.7$ and $\pi_1 = 33$ given in (5), increases ants interference with predators. Ants forage exclusively on prey resources when $P \ge \pi_1$, maximizing predation interference and prey-predator interaction strength. The thickness of arrows corresponds with the interaction strength. Parameters used in this simulation are from Table 1 with $F = 2.2$ and $M = 50$.

In the case of mutualistic interactions, ants obtain energetic benefits in the form of food, and in return provide services to their partners (e.g., fungus gardening [54]; hygiene [6]; pollination [15]). One of the most important services that ants can provide is defense against their partners' natural enemies. Such is the case of ant–plant mutualisms where ants interfere with plant's herbivores [23], or ant–insect mutualisms in which ants protect aphids [48] and other insects from predators and parasitoids. In the case of ant–plant mutualisms, ants are attracted by *nectar* supplied through special plant organs, e.g., *nectaries*. Many plants also provide shelter to their ant defenders. In the case of ant–insect mutualisms, ants are attracted by the *honeydew* secreted by prey such as aphids, scale insects, and some butterfly larvae [49].

This form of mutualism in which at least three species participate (e.g., victim, exploiter & ant), is a subject of the great interest for ecology [38] and agriculture [37,51]. Such complex interactions were studied using a variety of models, e.g., system of differential equations [2,10,40], spatio–temporal models [50], and by means of a board game in one instance [12]. Since ants are adaptive foragers [52,53], evolutionary game theory (EGT) can help us to understand the dynamics of ant-defense mutualisms when multiple food types for ants are available. EGT postulates than when facing alternative sources of food, consumers (here ants) distribute their foraging effort such that individual fitness maximizes [27]. In the absence of other constraints, this leads to the ideal free distribution of foraging preferences [IFD; 11], where the number of consumers for each resource type is proportional to the resource's *profitability*, where profitability comprises both *availability* (e.g., amount, supply rate) and *quality* (e.g., calories, nutrient ratios) of the resource.

In this article we study the consequence of ant optimal foraging for defense mutualism, where the defended species (hereafter the "prey") can be either a plant or an insect herbivore (e.g., aphids), and the enemy (hereafter the "predator") can be an insect herbivore (e.g., aphids) or an insect carnivore (e.g., ladybugs). Rather than dealing with an explicit three variable model for the populations of prey, predators and ants, we consider a two-species prey–predator model, with variable predation interference by a fixed size ant population. This approach allows us to demonstrate the effects of adaptive ant protection mutualism on prey–predator population dynamics. We show that adaptive ant protection mutualism allows coexistence of predators and prey at alternative equilibria, along limit cycles, or a combination of both. These results can be useful to understand and predict effects of manipulations of ant defensive mutualism, by supplying artificial food sources in agricultural systems [36,37].

2. Models and methods

We consider a community module consisting of *prey* with population density P, *predators* with density H, and a colony of *mutualists* of size M. Mutualists weaken the prey–predator interaction strength, e.g., by interfering with predators or actively deterring predators. The level of interference depends on the *preference* $0 \le u \le 1$ of mutualists for resources produced by the prey, versus $1 - u$ for *alternative* food sources provided at a fixed rate F (see the three inset interaction graphs in Fig. 1). If mutualists specialize on alternative resources ($u = 0$, left graph), predator-prey interactions are strongest because prey are not protected at all (interaction strength between prey and predators is shown by the thickness of the $P \to H$ arrow in Fig. 1). When mutualists are generalist foragers ($0 < u < 1$, middle graph), the interaction strength as well as prey

Table 1
Variables and parameters used in simulations.

Symbol	Description	Default value
P	prey population density (time dependent)	–
H	predator population density (time dependent)	–
u	ant preference for the prey resources (time dependent)	–
M	ant colony size	various values
r	prey's intrinsic growth rate	0.1
K	prey's environmental carrying capacity	50
a	maximum predation rate	0.01
e	predator's conversion efficiency	0.5
m	predator's intrinsic mortality rate	0.05
q	strength of ant interference on predation	various values
s	prey resource supply rate (per capita)	0.1
F	alternative resource supply rate	various values
w	resource loss rate	0.1
b	ant's specific consumption rate	0.001

protection is intermediate, and when mutualists specialize on the prey resource ($u = 1$, right graph), the interaction strength is weakest because the protection level is highest. The best known example of such a community consists of aphids (prey), coccinellids (predators), and ants that protect aphids. Alternatively, we can consider plants (prey), aphids (predators), and ants that protect plants. For this reason we refer in this article to the mutualist as ants. In these systems prey secretions (i.e., plant's nectar, aphid's honeydew) compete with alternatives (e.g., other plants/aphids, artificial sources) for ant's preferences, affecting the quality of the mutualistic service.

We model the dynamics of the *prey–predator–ant* system through the feedback between prey–predator population dynamics and adaptive foraging preferences by ants by assuming that ants are optimal foragers that instantaneously maximize their fitness at current prey and alternative resource densities. Section 2.1 describes how ant preferences affect prey and predator population dynamics, while Section 2.2 describes how ant's foraging preferences depend on the primary prey and the alternative resource densities. Combination of these mechanisms leads to a non-smooth dynamic model whose equilibria we analyze in Section 3. In Section 4 we analyze the model numerically with respect to changes in alternative resource density and ant colony size.

2.1. Prey–predator dynamics

We consider variable prey P and predator densities H following the Lotka–Volterra (LV) equations

$$\frac{dP}{dt} = rP\left(1 - \frac{P}{K}\right) - \frac{aPH}{1 + quM} \tag{1a}$$

$$\frac{dH}{dt} = \frac{eaPH}{1 + quM} - mH, \tag{1b}$$

where r is the prey per capita population intrinsic growth rate, and K is the environmental carrying capacity. Predation takes place with the maximum specific rate a without ant interference. Predators convert eaten prey into new births with efficiency e, and decline with mortality rate m. A fraction u ($0 \le u \le 1$) of the ant colony forages on prey supplied resources (i.e., plant's nectar, aphid's honeydew). Foraging ants defend prey by attacking, evicting or threatening predators, decreasing prey exploitation with a strength modeled by the interference constant q. Thus, ant preference u is also a proxy for the*protection level* that prey receive from the ants, i.e., $u = 0$ means the prey is "not protected", $u = 0.5$ means it is "half-protected", and $u = 1$ means it is "maximally protected".

We assume that both ant colony size (M) and the supply rate of alternative sources (F) are fixed parameters of the model that can be manipulated. On the other hand, we consider ant foraging preference u as an adaptive trait that varies in response to changes in prey density P caused by dynamics (1). Although M is fixed, the effective size of the ant's colony (uM) affecting the prey–predator interaction strength can vary between 0 and M.

We stress that Eq. (1) is the Lotka–Volterra predator-prey model when ant preferences for prey are fixed. Thus, for fixed u dynamics of (1) always converge to a globally stable equilibrium. For $K < m(1 + quM)/(ae)$ only prey survive at the equilibrium $(P, H) = (K, 0)$, while for $K > m(1 + quM)/(ae)$ both prey and predators coexist at globally stable equilibrium

$$(P, H) = \left(\frac{m(Mqu + 1)}{ae}, \frac{r(Mqu + 1)(aeK - mMqu - m)}{a^2 eK}\right).$$

As we will see in Section 2.2, when ants are optimal foragers, their preference u for prey will become a function of the prey density, which makes model (1) highly nonlinear and with rich set of attractors.

2.2. Adaptive ant preferences

Let us assume that ants feed on prey (P) supplied resources with preference u and on alternative resources (F) with preference $1-u$. The payoff U (V) that an ant obtains when foraging on resources supplied by P (F) depends on supply vs. consumption balances and on the distribution of the colony foraging preferences. Appendix A shows that these payoffs are

$$U = \frac{sP}{w + buM}, \quad V = \frac{F}{w + b(1-u)M}, \tag{2}$$

where s is the prey per capita resource supply or secretion rate, b is the specific ant consumption rate of the resource, and w is the loss rate of unconsumed resources (e.g., evaporation, re-absorption, or consumed by a different consumer).[1] Since survival and reproduction of ants depends on resource consumption we define a proxy for ant fitness as the average payoff

$$W = u\left(\frac{sP}{w + buM}\right) + (1-u)\left(\frac{F}{w + b(1-u)M}\right). \tag{3}$$

Next, we consider the optimal preference u that maximizes ant fitness for given prey population abundance P, alternative resource supply rate F, and ant colony size M. Calculations in Appendix A show that the *evolutionarily stable strategy* (ESS) for fitness (3) is

$$u = \begin{cases} 0 & \text{if } \ P \le \pi_0 \\ \dfrac{sP}{sP+F} + \dfrac{w(sP-F)}{b(sP+F)M} & \text{if } \ \pi_0 < P < \pi_1 \\ 1 & \text{if } \ P \ge \pi_1, \end{cases} \tag{4}$$

where

$$\pi_0 = \left(\frac{w}{w + bM}\right)\frac{F}{s} \tag{5a}$$

$$\pi_1 = \left(\frac{w + bM}{w}\right)\frac{F}{s}, \tag{5b}$$

are prey density thresholds at which ant foraging switches between specialization and generalism. When prey density is below π_0, prey resource supply is too low and it is better for ants to switch entirely to alternative resources, thus $u = 0$. Above π_1 the ants do the opposite and forage exclusively on the resource provided by the prey, i.e., $u = 1$. Between these critical values, ant preference for the prey resource increases with prey density P, see Fig. 1. Because $\frac{\partial^2 u}{\partial P^2} = -\frac{2Fs^2(bM+2w)}{bM(F+Ps)^3} < 0$ for $\pi_0 < P < \pi_1$, $u(P)$ is concave in this interval. As ant population M increases to infinity, $\pi_0 \to 0$ and $\pi_1 \to \infty$, and ant preference for the prey resource converges to $\frac{sP}{sP+F}$. In this case ant preferences for the two resources match supply resource ratio $\frac{u}{1-u} \approx \frac{sP}{F}$ which is called the Parker's matching principle [39], a special case of the Ideal Free Distribution [27].

Thus, our model combines predator-prey population dynamics described by Lotka–Volterra Eq. (1) and ant preferences ESS (4) that track instantaneously predator and prey population densities. This corresponds to time scale separation, where ant foraging behavior operates on a much faster time scale when compared to predator-prey population dynamics. Thus, changes in predator and prey population densities drive ant foraging preferences that, in turn, influence population dynamics, leading to a complex feedback between ant behavior and demography. In Section 3 we analyze conditions for equilibrium existence and stability, and in Section 4 we study population-preference dynamics as a function of F and M using numerical methods of bifurcation analysis. Table 1 gives a complete list of all model parameters together with their values.

Equations in (1) with preferences given in (4) form a *piecewise-smooth system* [47], where the right-hand-side of (1) is continuous in state variables, but its Jacobian is not defined at thresholds π_0 and π_1 (5). This also happens in other consumer preference models [41–43], where preferences are piecewise continuous, or in harvesting models where harvesting rates are piecewise continuous [55]. In contrast, when controls such as adaptive preferences [28] or harvesting rates [56] have "jump" discontinuities, we have a *Filippov system* where dynamical phenomena such as *sliding* can occur [5,9].

3. Equilibria and local dynamics

System (1) has a *trivial* equilibrium $(P, H) = (0, 0)$ and a *prey-only equilibrium* $(K, 0)$. In the absence of ant adaptation, i.e., assuming fixed u, a single *coexistence equilibrium* $P^* > 0, H^* > 0$ can exist at the intersection of prey and predator isoclines [4,35]. By setting $\frac{dP}{dt} = \frac{dH}{dt} = 0$ in (1), we get non-trivial isoclines

$$H = \frac{r(1 + quM)}{a}\left(1 - \frac{P}{K}\right) \tag{6a}$$

[1] For simplicity we assume the same values of b and w for both ant food sources, implying a similar resource ecology.

$$P = \frac{m(1+quM)}{ea}, \tag{6b}$$

for prey and predators, respectively. The prey isocline (6a) is a decreasing line intersecting the prey axis at $P = K$ and the predator axis at $H = \frac{r(1+quM)}{a}$, respectively. The predator isocline (6b) is a line parallel to the predator axis. If $K > P^* = \frac{m(1+quM)}{ea}$ the isoclines intersect at interior predator-prey equilibrium

$$(P^*, H^*) = \left(\frac{m(1+quM)}{ea}, \frac{r(1+quM)}{a}\left(1 - \frac{m(1+quM)}{eaK}\right)\right) \tag{7}$$

which is globally asymptotically stable [4,35]. We observe that as the ant preference u for the prey resource increases, the prey population density increases too, due to increased protection of prey by ants. On the other hand, dependence of predator equilibrium density on ant preference u is quadratic with maximum at $u = \frac{aeK-2m}{2mMq}$ provided $\frac{2m}{ae} < K < \frac{2m(Mq+1)}{ae}$. For smaller values of M satisfying $K > \frac{2(mMq+m)}{ae}$, the maximum predator equilibrium density is reached when $u = 1$. On the other hand, when $K < \frac{2m}{ae}$, maximum predator equilibrium density is reached at $u = 0$. This non-monotonic response of the predator equilibrium density on u is a consequence of two opposite mechanisms. First, as ant interference increases (i.e., as quM increases), equilibrium prey density increases which also leads to increase in the predator population size. Second, increased ant interference decreases predator attack rate $\frac{aP}{1+quM}$. Combination of these two mechanisms leads to the hump-shaped dependence of the predator equilibrium population size on ant interference.

In the next section we show the effects of adaptive ant foraging behavior on prey and predator isoclines and stability.

3.1. Prey and predator isoclines under adaptive ant preference

Now we assume that ant preference for the prey resource u, given in (4), tracks instantaneously current prey and predator population densities and we study the feedback between rapid ant adaptation and predator-prey population dynamics. Since ant preference is a continuous, non-linear function of prey density P and it is defined piece-wise, we show that isoclines are defined piece-wise too and *multiple coexistence equilibria* are possible.

First we study the non-trivial predator isocline which is formed by points in the prey-predator phase space that satisfy $\frac{dH}{Hdt} = 0$ in (1b) with u given in (4). This equation has up to four solutions

$$P_0^* = \frac{m}{ea} \quad \text{if } P_0^* \le \pi_0 \tag{8a}$$

$$P_-^* = \frac{ms(bMq+b+qw) - abeF - \sqrt{(ms(bMq+b+qw) - abeF)^2 + 4abeFms(b-qw)}}{2beas} \quad \text{if } \pi_0 < P_-^* < \pi_1 \tag{8b}$$

$$P_+^* = \frac{ms(bMq+b+qw) - abeF + \sqrt{(ms(bMq+b+qw) - abeF)^2 + 4abeFms(b-qw)}}{2beas} \quad \text{if } \pi_0 < P_+^* < \pi_1 \tag{8c}$$

$$P_1^* = \frac{m(1+qM)}{ea} \quad \text{if } P_1^* \ge \pi_1 \tag{8d}$$

where $P_0^* < P_1^*$ and $P_-^* \le P_+^*$, provided P_-^* and P_+^* are real. It is proved in Appendix B that at most three of the four solutions can be positive for a given set of parameter values. This shows that the predator non-trivial isocline can consists of maximum three segments that are vertical lines in the prey-predator phase space (see the vertical solid lines in Fig. 2). The following cases are possible (see Appendix B):

Case 1: $\pi_0 < P_0^*, \pi_1 < P_1^*$: the predator isocline consists of single segment $P = P_1^*$ (Fig. 2a).
Case 2: $\pi_0 > P_0^*, \pi_1 > P_1^*$ and

a: P_-^* and P_+^* are real: the predator isocline consists of three vertical segments $P = \{P_0^*, P_-^*, P_+^*\}$ (Fig. 2b).
b: P_-^* and P_+^* are not real: the predator isocline consists of single segment $P = P_0^*$ (Fig. 2c).

Case 3: $\pi_0 < P_0^*, \pi_1 > P_1^*$: the predator isocline consists of single segment $P = P_+^*$ (Fig. 2d).
Case 4: $\pi_0 > P_0^*, \pi_1 < P_1^*$: the predator isocline consists of three segments $P = \{P_0^*, P_-^*, P_1^*\}$ (Fig. 2e).

Different segments of the predator isocline correspond to qualitatively different ant preferences for the prey resource. Segments at P_0^* (8a) and P_1^* (8d) correspond to lowest and highest values of prey equilibrium density, where ants specialize on alternative resources ($u = 0$) or prey resources ($u = 1$), respectively. Segments of the predator isocline at P_-^* and P_+^* (8b), (8c) correspond to intermediate predator preference for prey and alternative resources ($0 < u < 1$).

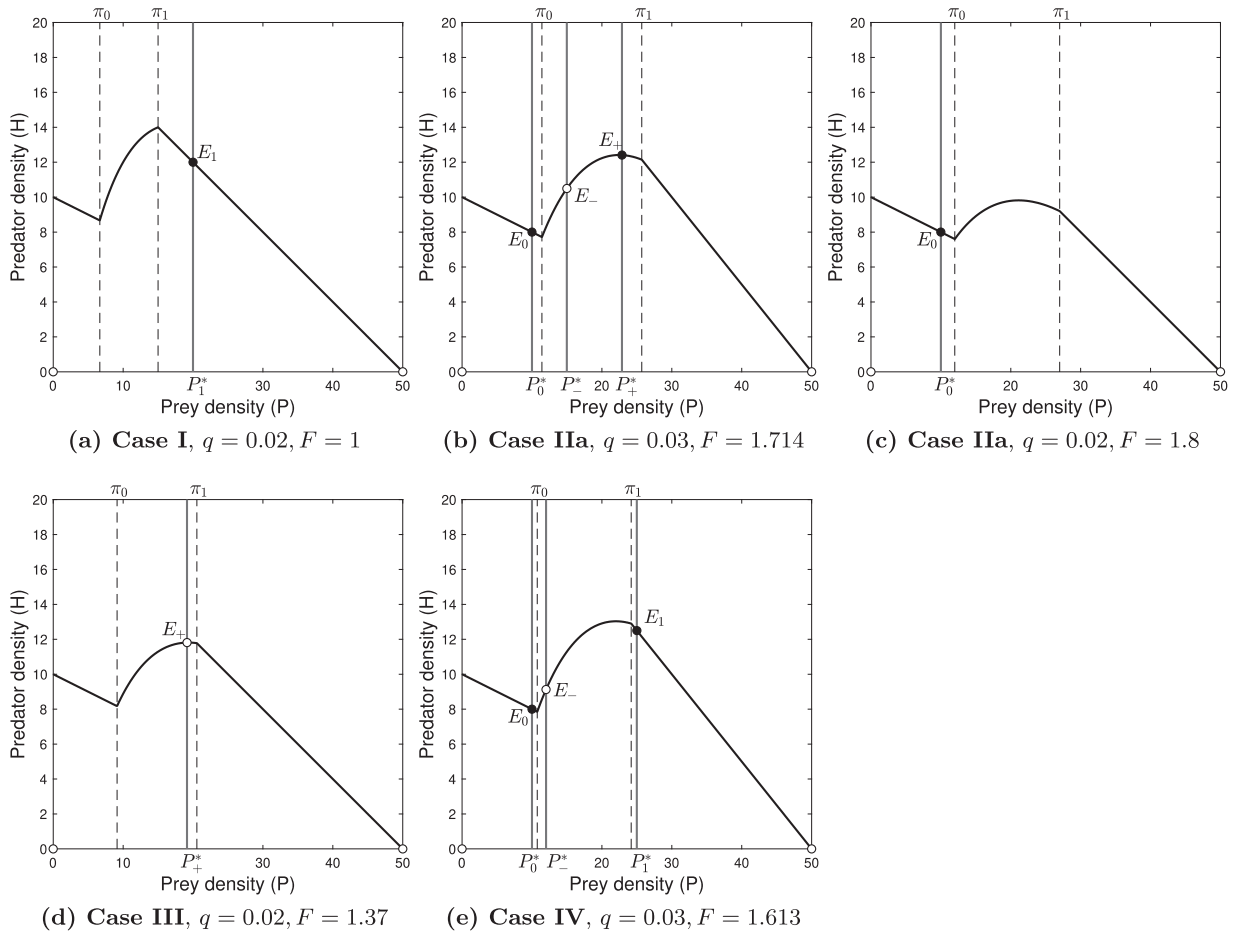

(a) **Case I**, $q = 0.02, F = 1$ (b) **Case IIa**, $q = 0.03, F = 1.714$ (c) **Case IIa**, $q = 0.02, F = 1.8$

(d) **Case III**, $q = 0.02, F = 1.37$ (e) **Case IV**, $q = 0.03, F = 1.613$

Fig. 2. Isoclines of system (1) under adaptive ant preference (4). Equilibria $E_i = (P_i^*, H_i^*)$ lie at intersections of the prey isocline (9) (black solid curve) and segments of the predator isocline at $P = P_i^*$ (8) (gray vertical lines). Black dots (circles) represent stable (unstable) equilibria. Dashed lines indicate $P = \pi_0$ and $P = \pi_1$ thresholds (5). Parameters used in panels are those given in Table 1 with $M = 50$ and q, and F indicated below each panel.

Second, the non-trivial prey isocline satisfies $\frac{dP}{Pdt} = 0$ in (1a) with $u(P)$ given in (4). As a result, prey isocline $H = \Gamma(P)$ is a continuous, piece-wise defined function

$$\Gamma(P) := \begin{cases} \dfrac{r(K-P)}{aK} & \text{if } P \le \pi_0 \\ \dfrac{r(K-P)}{aK}(1+qMu(P)) & \text{if } \pi_0 < P < \pi_1 \\ \dfrac{r(K-P)}{aK}(1+qM) & \text{if } P \ge \pi_1, \end{cases} \tag{9}$$

shown as the black curve in Fig. 2. We observe that prey isocline segments for $P \le \pi_0$ and $P \ge \pi_1$ are linearly decreasing with prey density, and the second segment decreases faster than the first segment. Because we know that $u(P)$ is increasing (i.e., $du/dP > 0$) and concave (i.e., $d^2u/dP^2 < 0$) for $\pi_0 < P < \pi_1$, we get $\frac{d^2\Gamma}{dP^2} = \frac{rqM}{aK}\left((K-P)\frac{\partial^2 u}{\partial P^2} - 2\frac{\partial u}{\partial P}\right) < 0$ for $P < K$, i.e., the segment of the prey isocline for $P \in [\pi_0, \pi_1]$ is concave too. The prey isocline is continuous, with values $\Gamma(\pi_0) = \frac{r(K-\pi_0)}{aK}$ and $\Gamma(\pi_1) = \frac{r(1+qM)(K-\pi_1)}{aK}$. Depending on K and thresholds π_0 and π_1, $\Gamma(P)$ has the following number of pieces in the positive part of the prey–predator phase plane: (i) if $K > \pi_1$ the prey isocline consists of three pieces, i.e., $P \le \pi_0$, $\pi_0 < P < \pi_1$ and $P \ge \pi_1$; (ii) if $\pi_0 < K < \pi_1$ the prey isocline consists of two pieces $P \le \pi_0$ and $\pi_0 < P < \pi_1$; and (iii) if $K < \pi_0$ the prey isocline consists of $P \le \pi_0$ piece only which is linear. In all three cases the prey isocline intersects the H-axis at $H = \frac{r}{a}$ and the P-axis at $P = K$. Prey density increases in the region below the isocline, i.e., where $H < \Gamma(P)$, and decreases in the region above where $H > \Gamma(P)$. Fig. 2 shows the case where $\pi_1 < K$ and the prey isocline consists of three pieces.

3.2. Equilibria and local stability

Coexistence equilibria $E_i := (P_i^*, H_i^*)$ correspond to intersections of prey and predator isoclines. Sub-index $i = 0$, 1, –, + indicates whether ants specialize on alternative resources ($i = 0$), prey resources ($i = 1$), or consume both resources ($i = -$ or $i = +$). At an equilibrium prey density P_i^* is given in (8) and predator density $H_i^* = \Gamma(P_i^*)$ in (9). From (9) coexistence requires that $P_i^* < K$, i.e., the prey equilibrium density cannot be higher than is the environmental carrying capacity. In addition, the existence of E_0, E_1, E_- or E_+ in the first quadrant of the prey–predator phase plane also depends on the supply rate of alternative resources F and colony size M, which control ant preferences u given in (4). Now we classify coexistence equilibria as a function of K, F and M.

Equilibrium E_0 in which ants specialize on alternative resources ($u = 0$)

$$E_0 = (P_0^*, H_0^*) = \left(\frac{m}{ea}, \frac{r(eaK - m)}{ea^2K}\right), \tag{10}$$

exists provided (i) $P_0^* < \pi_0$ and (ii) $P_0^* < K$. Using (5a) and (8a) condition (i) becomes

$$F > \phi_0(M) := \frac{sm(w + bM)}{eaw}, \tag{11}$$

and (ii) becomes

$$\frac{m}{ea} < K. \tag{12}$$

Equilibrium E_1 in which ants specialize on resources supplied by prey ($u = 1$)

$$E_1 = (P_1^*, H_1^*) = \left(\frac{m(1 + qM)}{ea}, \frac{r(1 + qM)(eaK - m(1 + qM))}{ea^2K}\right), \tag{13}$$

exists provided (i) $P_1^* > \pi_1$ and (ii) $P_1^* < K$. Using (5b) and (8d) condition (i) becomes

$$F < \phi_1(M) := \frac{smw(1 + qM)}{ea(w + bM)}, \tag{14}$$

and (ii) becomes

$$M < \frac{aeK - m}{mq}. \tag{15}$$

Equilibria E_- and **E_+** in which ants are generalists ($0 < u < 1$)

$$E_- = (P_-^*, H_-^*) = \left(\frac{m(1 + qu(P_-^*)M)}{ea}, \frac{r(1 + qu(P_-^*)M)\big(eaK - m(1 + qu(P_-^*)M)\big)}{ea^2K}\right) \tag{16}$$

$$E_+ = (P_+^*, H_+^*) = \left(\frac{m(1 + qu(P_+^*)M)}{ea}, \frac{r(1 + qu(P_+^*)M)\big(eaK - m(1 + qu(P_+^*)M)\big)}{ea^2K}\right) \tag{17}$$

require that (i) P_-^*, P_+^* are real and (ii) $P_-^* < K$, $P_+^* < K$. Setting the square root in (8b) and(8c) equal to 0 condition (i) becomes

$$M > \frac{abeF - ms(b + qw) + 2\sqrt{abems(qw - b)F}}{bmsq}, \tag{18}$$

and after some algebra conditions (ii) can be rewritten as

$$M < \frac{b(eaK - m)(F + sK) + mqw(F - sK)}{bmqsK}, \tag{19}$$

for both P_-^* and P_+^*.

Notice that if (12) does not hold then (15) does not hold for $M \geq 0$ and E_1 is not feasible. From here onwards we will assume that (12) holds, i.e., the environmental carrying capacity K is large enough so that some interior equilibria exist. This means that prey are regulated by predators. Next, we use conditions (11), (14) and (18) to classify predator-prey equilibria with respect to the supply rate of alternative resources F and ant colony size M:

Case I: When alternative resource supply rate is low and satisfies $F < \min(\phi_0, \phi_1)$, there is only one coexistence equilibrium E_1 (13) where ants specialize on prey resources ($u = 1$). This corresponds to predator isocline **Case 1** where $\pi_0 < P_0^*, \pi_1 < P_1^*$: see Fig. 2a where a single predator isocline segment at P_1^* (8d) intersects the $P > \pi_1$ part of the prey isocline (9).

Case II: When alternative resource supply rate is high and satisfies $F > \max(\phi_0, \phi_1)$, there are two possibilities

a: If condition (18) is true, there are three coexistence equilibria $\{E_0, E_-, E_+\}$. At E_0 (10) ants prefer alternative resources exclusively ($u = 0$), at E_- (16) and at E_+ (17) ants consume both prey and alternative resources. This correspond to predator isocline **Case 2.a** ($\pi_0 > P_0^*, \pi_1 > P_1^*$, Fig. 2b) where the isocline segment at P_0^* (8a) intersects the $P < \pi_0$ part of the prey isocline, and the two segments at P_-^* (8b) and P_+^* (8c) intersect the $\pi_0 < P < \pi_1$ part of the prey isocline.

b: If condition (18) is false, there is one coexistence equilibrium E_0 where ants specialize on alternative resources ($u = 0$). This correspond to predator isocline **Case 2.b** ($\pi_0 > P_0^*, \pi_1 > P_1^*$, Fig. 2c) where the predator isocline segment at P_0^* intersects the $\pi_0 < P$ part of the prey isocline.

Case III: Alternative resource supply rate is intermediate and satisfies $\phi_1 < F < \phi_0$. There is only one coexistence equilibrium E_+ where ants are generalists ($0 < u < 1$). This correspond to predator isocline **Case 3** ($\pi_0 < P_0^*, \pi_1 > P_1^*$, Fig. 2d) where a single predator isocline segment at P_+^* intersects the $\pi_0 < P < \pi_1$ part of the prey isocline.

Case IV: Alternative resource supply rate is intermediate and satisfies $\phi_0 < F < \phi_1$. There are three coexistence equilibria $\{E_0, E_-, E_1\}$. At E_0 and E_1 ants specialize on alternative resources ($u = 0$) or prey resources ($u = 1$), respectively, at E_- ants are generalists ($0 < u < 1$). This correspond to predator isocline **Case 4** ($\pi_0 > P_0^*, \pi_1 < P_1^*$, Fig. 2e) where predator isocline segments at P_0^*, P_-^* and P_1^* intersect the $P < \pi_0$, $\pi_0 < P < \pi_1$ and $P > \pi_1$ parts of the prey isocline, respectively.

Like in standard prey–predator models, the geometry of isoclines intersections determines local stability of the prey–predator equilibrium. We assume that the prey equilibrium density is different from π_0 or π_1. This is because as we use linear stability analysis, we need that the right-hand side of model (1) is differentiable. A general result in predator-prey theory is that provided the prey isocline is decreasing at the equilibrium with prey density and the predator isocline is vertical, the equilibrium is locally asymptotically stable [4,26,35]. Thus, equilibrium states where ants specialize either on the alternative resource (E_0) or on the prey resource (E_1) are always locally asymptotically stable because at these points the prey isocline always decreases (see, e.g., E_1 in Fig. 2a and e and E_0 in Fig. 2b,c,e).

For equilibrium cases where ants are generalists, i.e., E_- or E_+, Appendix C shows that E_- is a saddle (e.g., Fig. 2b and e), and E_+ is unstable when the prey isocline is increasing at this equilibrium (e.g., Fig. 2d) or E_+ is locally stable when the prey isocline is decreasing (e.g., Fig. 2b).

4. Global predator-prey population & ant preference dynamics

In previous sections we showed how predator-prey equilibria change as ant colony size (M) and alternative resources supply rate (F) vary. We determine that local stability depends on the relative position of equilibria with respect to ant specialization–generalism thresholds $P = \pi_0$ and $P = \pi_1$ given in (5). This shows how global predator-prey population dynamics and ant preference dynamics change with F and M, using analytical methods. Now we will consider parameters from Table 1, at low ($q = 0.005$), moderate ($q = 0.02$), and strong ($q = 0.03$) ant interference on predation (see Appendix D for details) and in Section 4.1 we do bifurcation analysis along F gradient, and in Section 4.2 bifurcation analysis with respect to both F and M.

4.1. Effect of alternative resource supply F

Fig. 3 shows bifurcation diagrams of prey (left column) and predator (right column) densities with respect to increasing alternative resource supply rate F at fixed ant colony of size $M = 50$. Equilibria where predators specialize on the prey resource (E_1), or on the alternative resource (E_0) are independent of F and they are represented by horizontal line segments. At intermediate values of alternative resource supply F the two equilibria E_0 and E_1 are connected by a curve of equilibria corresponding to E_+ or E_-. The diagrams are divided by vertical lines at $F = \phi_0$ (11) and ϕ_1 (14) into four regions that correspond to the four cases in classification of predator-prey equilibria given in Section 3.2. Prey diagrams show ant preference thresholds π_0 and π_1 as a function of F (see dashed lines). The effect of F on the global dynamics varies greatly with the intensity of ant interference on predators q.

Weak ant interference ($q = 0.005$) Fig. 3 top row shows that equilibria E_1 and E_0 in regions **I** and **II** respectively, are connected by a curve of equilibria E_+ in region **III** where ants are generalist ($0 < u < 1$). E_1 is globally stable and coincides with E_+ at the threshold $F = \phi_1 \approx 0.84$. E_+ is globally stable up to $F \approx 1.184$ where a *super-critical Hopf bifurcation* **HB** occurs. This bifurcation gives rise to a *globally stable limit cycle* that annihilates as F approaches the **hb** point at $\phi_0 = 1.5$ boundary, where E_+ and E_0 coincide with the threshold π_0 at which population dynamics are non-smooth. The limit cycle dynamics for $F = 1.2$ (marked in Fig. 3a by the △ mark) is shown in Fig. 4a.

Moderate ant interference ($q = 0.02$) Fig. 3 middle row shows that increased ant interference leads to more complex predator-prey population dynamics. Like in the previous case, equilibrium E_1 in region **I** ($0 \le F \le \phi_1 = 1.33$) is globally stable. Equilibrium E_0 in region **II** ($F \ge \phi_0 = 1.5$) is locally stable, but the stability is not global. Equilibria E_1 and E_+ coincide at ϕ_1; E_0 and E_- coincide at ϕ_0, and equilibria E_- and E_+ collide and vanish at the saddle-node bifurcation **SN** ($F \approx 1.53$). Going left-to-right along the F axis illustrates transitions between equilibrium cases **I, III, II.a** & **II.b**: single equilibrium E_1 in region **I** is replaced by single equilibrium E_+ in region **III**, then follow equilibria $\{E_+, E_-, E_0\}$ in region **II**, until point **SN** from which on only E_0 remains.

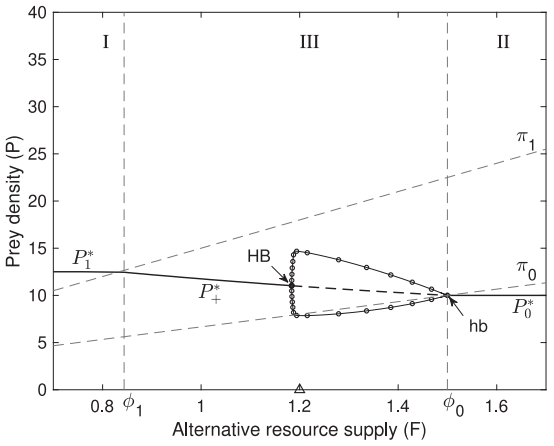

(a) $q = 0.005$

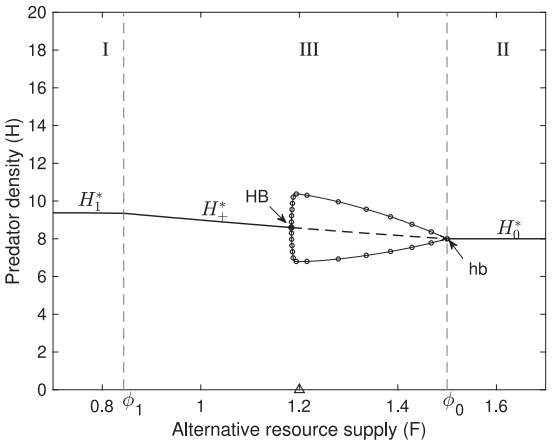

(b) $q = 0.005$

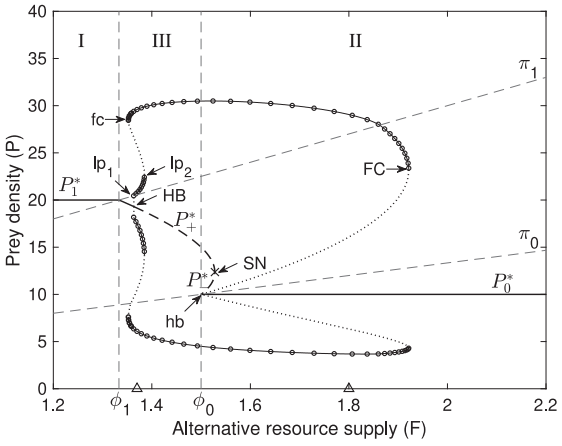

(c) $q = 0.02$

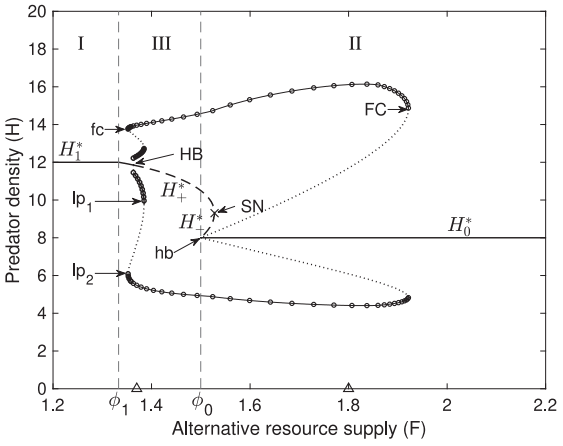

(d) $q = 0.02$

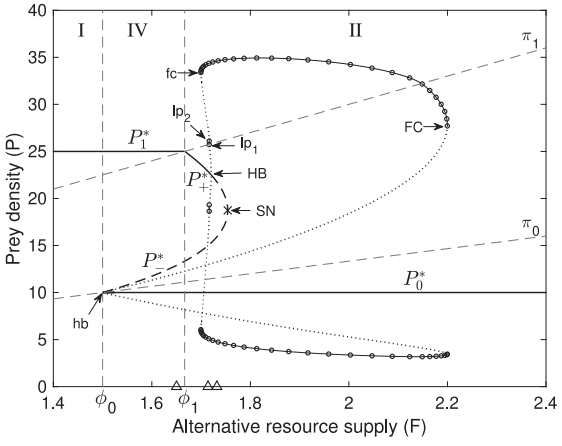

(e) $q = 0.03$

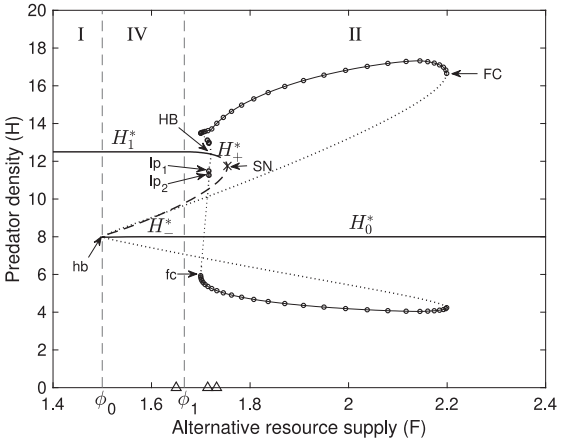

(f) $q = 0.03$

Fig. 3. Bifurcation diagrams with respect to alternative resource supply F at $M = 50$. Black solid (dashed) lines are stable (unstable) equilibria $E_i = (P_i^*, H_i^*)$. Lines with circles are stable limit cycles, and dotted lines are unstable limit cycles. **SN** stands for *saddle–node bifurcation*, **HB** & **hb** denote *Hopf bifurcation*, and **FC** & **fc** denote *fold bifurcation* of limit cycles. Limit cycles also fold at **lp1** and **lp2**. Vertical lines at $F = \phi_0$ and ϕ_1 (11), (14), dashed) separate equilibrium cases **I, II, III, IV**. Increasing lines π_0 and π_1 (dashed, left column only) are ant specialization and generalism thresholds (5). Parameters from Table 1; q indicated on the labels; triangles (△) indicate F-values considered by Fig. 4.

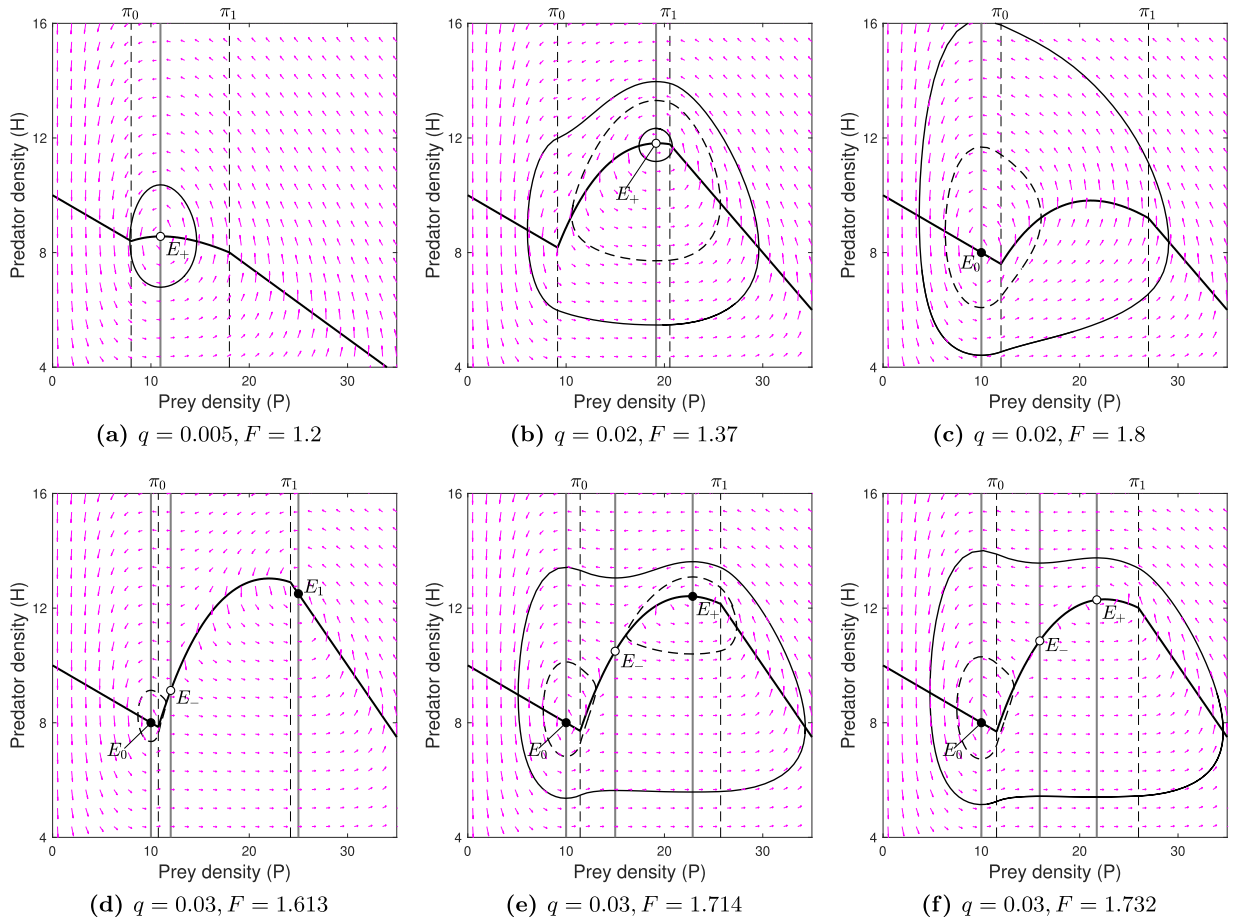

Fig. 4. Global dynamics predicted by Fig. 3 for $M = 50$. Locally stable equilibria are shown as dots, unstable equilibria as circles. Locally stable limit cycles (solid curves) are shown together with unstable cycles (dashed curves). Parameters are taken from Table 1 with q and F given below panels.

As F increases, equilibrium E_+ loses its stability at *a super-critical* **HB** ($F \approx 1.36$) giving rise to *stable and unstable limit cycles*. Unlike the case of Fig. 3a and b where the limit cycle is globally stable and restricted to region **III**, Fig. 3c and d displays a branch of limit cycles spanning regions **III** and **II**, from point **HB** to point **hb** where E_0 and E_- coincide at ϕ_0. Limit cycles switch orientation and stability at several folding points **lp1** ($F \approx 1.363$), **lp2**($F \approx 1.385$), **fc** ($F \approx 1.352$) and **FC**($F \approx 1.921$). Thus, there are two sub-branches of locally stable limit cycles: the short one **lp1–lp2** and the longest one **fc–FC**. And there are three unstable sub-branches of limit cycles: two short ones **lp1–HB** and **fc–lp2** and the longest one **hb–FC**.

Unstable limit cycles delineate boundaries of several attractors in the prey–predator phase plane. For example, Fig. 3c and d shows that both locally stable limit cycles branches overlap with the unstable cycle branch **lp1–lp2** at $1.363 < F < 1.385$, and Fig. 4b shows the corresponding population dynamics at $F = 1.37$ (marked in Fig. 3c and d by the $\triangle$ mark), where unstable equilibrium E_+ is surrounded by two stable limit cycles separated by an unstable cycle. Thus, a moderately small perturbation of point E_+ leads to low amplitude oscillations, but initial conditions far enough from E_+ (e.g., near (0,0) or $(K, 0)$) lead to large amplitude oscillations instead. An unstable cycle also causes equilibrium E_0 to be only locally stable between **hb** and **FC** ($1.5 < F < 1.921$), and globally stable beyond **FC** where limit cycles do not exist anymore ($F > 1.921$). Fig. 4c documents predator-prey dynamics at $F = 1.8$ (denoted by the right $\triangle$ mark in Fig. 3c and d), where the unstable limit cycle separates domains of attraction of equilibrium E_0 and the large amplitude oscillation limit cycle.

Strong ant interference ($q = 0.03$) Fig. 3 bottom row displays an important difference with previous cases. When ant interference is strong, $\phi_0 = 1.5 \leq \phi_1 \approx 1.667$, which contrasts with the previous cases where $\phi_1 < \phi_0$. Like in the condition of moderate interference ($q = 0.02$), there is a continuous curve of equilibria where E_1 changes to E_+ at $F = \phi_1$, E_+ changes to E_- at **SN** ($F \approx 1.754$), and E_- changes to E_0 at **hb** ($F = \phi_0$). This time however, going left-to-right along the F axis illustrates transitions between equilibrium cases **I, IV, II.a** & **II.b** because the globally asymptotically stable equilibrium E_1 in region **I** is followed by three equilibria $\{E_1, E_-, E_0\}$ in region **IV**, then by three equilibria $\{E_+, E_-, E_0\}$ in region **II**, until point **SN** from which only E_0 remains.

Here again the bifurcation diagram predicts multiple stable and unstable limit cycles. The branch of limit cycles spans regions **IV** and **II**, connecting points **HB** and **hb** and switching orientation and stability at several folding points **lp1**($F \approx 1.716$), **lp2** ($F \approx 1.716$), **fc**($F \approx 1.699$) and **FC** ($F \approx 2.2$). Unstable limit cycles originate in region **IV** at the **hb** point ($F = \phi_0$), where equilibria E_0 and E_- coincide and the prey density is equal to π_0. At this point population dynamics are non-smooth. This is well below the **HB** point ($F \approx 1.72$) where E_+ loses stability in region **II**. Fig. 3e and f show that limit cycles are always unstable in region **IV**, and stable limit cycles occur only in region **II**.

For $\phi_0 < F < \phi_1$, Fig. 4d ($F = 1.613$ indicated by the left $\triangle$ mark in Fig. 3e and f) shows that the unstable limit cycle in region **IV** separates the regions of attraction of equilibria E_0 and E_1. Initial conditions inside the cycle lead towards E_0 while initial conditions outside lead towards E_1. For $F > \phi_1$ we have two interesting examples from region **II** where existence of two unstable limit cycles leads to alternative states, either a stable coexistence at equilibrium E_0 or E_+, or non-equilibrium coexistence along a locally stable large amplitude limit cycle. Fig. 4e illustrates the dynamics for $F = 1.714$ (indicated by the middle $\triangle$ mark in Fig. 3e and f) in the narrow interval between **fc** and **lp2**, where points E_0, E_-, E_+ occur together with two unstable limit cycles and one stable limit cycle. Initial conditions inside one or the other unstable limit cycle lead towards stability at equilibrium E_0 or E_+, but initial conditions outside of both cycles lead towards large amplitude predator-prey oscillations along the locally stable limit cycle. A small increase in alternative resource supply rate to $F = 1.732$ (indicated by the right $\triangle$ mark in Fig. 3e and f) destabilizes E_+ and the limit cycle centered at this equilibrium disappears (Fig. 4f). Qualitatively, the global dynamics are similar to the situation in Fig. 4c.

Fig. 3a,c,e shows that the maximum amplitude of locally stable limit cycles increases with q. As ant interference increases, oscillations cause ant preferences to vary periodically between specialization and generalism. This happens at those values of F where minima or maxima of limit cycles cross π_0 and/or π_1 threshold lines. This is also documented in Fig. 4 when the locally stable limit cycle crosses these thresholds.

Finally, Fig. 3 shows that as q increases locally stable limit cycles continue to exist for higher F-values. For $q = 0.005$ stable oscillations only occur if $F < \phi_0 = 1.5$, for $q = 0.02$ they occur for $1.352 < F < 1.921$, and for $q = 0.03$ for $1.699 < F < 2.2$.

4.2. Effect of ant colony size M

Fig. 5 shows which attractors, *locally stable equilibria* or *locally stable limit cycles*, occur at different combinations of alternative resource supply rate F and ant colony size M for weak ($q = 0.005$), intermediate ($q = 0.02$), and strong ($q = 0.03$) level of ant interference on predation. The ϕ_0 (11) line (dashed) and ϕ_1 (14) curve (dashed) divide the F vs. M parameter space in up to four regions **I, II, III** and **IV** corresponding to equilibrium cases **I, II, III** and **IV**, respectively, from Section 3.2. We observe that ϕ_0 is a line with a positive slope while ϕ_1 is a hyperbola. As q increases, the slope of ϕ_1 changes from decreasing (Fig. 5a) to increasing (Fig. 5b and c). Both lines intersect at $(M, F) = \left(0, \frac{sm}{ea}\right)$, and, provided $qw > 2b$, at $(M, F) = \left(\frac{w(qw-2b)}{b^2}, \frac{ms(qw-b)}{abe}\right)$ (Fig. 5c). The plane is further divided by curves corresponding to saddle–node bifurcations **SN** (solid red), Hopf bifurcations **HB** (solid blue) and fold points of limit cycles **fc** and **FC** (solid black) from Fig. 3 (the **hb** line coincides with ϕ_0).

Weak ant interference ($q = 0.005$) For this condition Fig. 5a shows regions **I, III** and **II**, corresponding to coexistence at E_1, E_+ and E_0, respectively, i.e., equilibrium cases **I, III** and **II.b**, respectively. Coexistence is stable for most F and M combinations except for the part of region **III** between the **HB** and ϕ_0 lines where a globally stable limit cycle occurs (cf. Fig. 3a).

Moderate ant interference ($q = 0.02$). For this condition Fig. 5b shows regions **I, III** and **II** again, but predator-prey population dynamics are considerably more complex. Whereas regions **I** and **III** correspond to equilibrium cases **I** and **III** (with locally stable equilibria E_1 and E_+, respectively), region **II** covers equilibrium cases **II.a** and **II.b**: there are two locally stable equilibria E_+ and E_0 between ϕ_0 and **SN** lines, or only E_0 below the **SN** line. Thus, equilibrium E_+ and Hopf bifurcations **HB** exist in regions **III** and **II**. In contrast with Fig. 5a where limit cycles reside entirely in region **III**, Fig. 5b shows that stable limit cycles bounded by ϕ_1, **fc** and **FC** lines span regions **III** and **II**.

Strong ant interference ($q = 0.03$) Fig. 5c shows that all four parameter regions **I** to **IV** with qualitatively different equilibria can co-exist. There is a gray region where coexistence between prey and predators is not possible because conditions (15) and (19) are not met and predators are not viable (this region is above $M = 150$, thus not displayed in Fig. 5a and b). In contrast with previous Fig. 5b, in this bifurcation diagram Hopf bifurcations (**HB**) and stable limit cycles occur in region **II** only, bounded by the ϕ_1, **fc** and **FC** lines. There are limit cycles in region **IV**, but they are unstable.

To sum up, Fig. 5 shows that increasing ant colony size M increases the number of parameter combinations where prey get stable protection from predation, either fully, like in equilibrium E_1 where ants specialize on prey resources ($u = 1$), or partially like in E_+ where ants are generalists and forage on prey and alternative food resources ($0 < u < 1$). When q is large enough, the full protection at E_1 is only locally stable in region **IV**, but Figs. 3e,f and 4 d indicate that the equilibrium without protection at E_0 has a very small attraction region. Finally, Fig. 5b and c shows that ant interference extends to non-equilibrium conditions via a limit cycle along which ant foraging preference changes periodically. As a result, outcomes without any prey defense from predation, i.e., E_0 where $u = 0$, are globally stable only below the **FC** line in region **II**. Indeed, as ant interference strength (q) increases, the area of global stability for E_0 on parameter space F vs. M decreases, from the totality of region **II** to only a part of it.

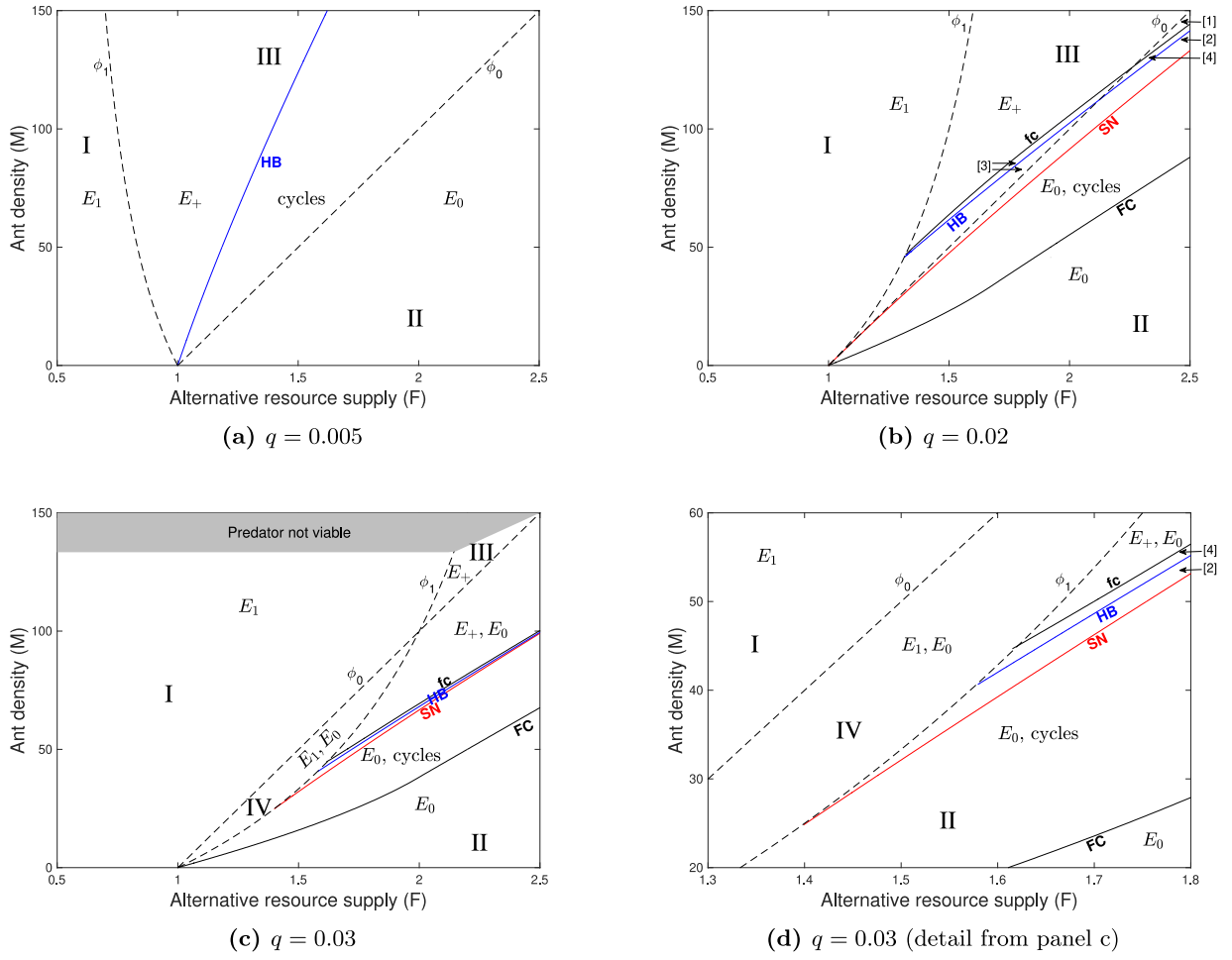

Fig. 5. 2D bifurcation diagram for prey-predator dynamics with adaptive ant foraging preference with respect to the alternative resource supply rate F and the ant colony size M. Dashed lines ϕ_0 (11) and ϕ_1 (14) divide the $M-F$ plane in four regions (**I, II, III, IV**) depending on whether ants behave as generalists or specialists at the corresponding predator-prey equilibrium. **SN** (red line) denotes the saddle–node bifurcation, **HB** (blue line) denotes the Hopf bifurcation, **fc** & **FC** (black lines) denote folds of limit cycles (see Fig. 3). E_0, E_1, E_+ and "cycles" indicate a region's attractor(s). Small regions are numbered: [1] = [E_0, E_+], [2] = [E_0, cycles], [3]=[E_+, cycles], [4] = [E_0, E_+, cycles]. A portion of panel (c) is expanded in panel (d) to help visualize the **HB** line between **fc** and **SN**. The gray area denotes the set of parameters at which no predator-prey coexistence is possible due to low environmental carrying capacity K, i.e., at these parameter values inequalities given in (19) and (15) do not hold. Parameters are taken from Table 1 with values of q indicated below panels.

5. Discussion

This article studies effects of mutualisms based on exchange of resources for defense, protection or deterrence against predation on predator-prey population dynamics. Our study demonstrates that interference of adaptive mutualists with predator-prey population dynamics leads to complex dynamics, including coexistence at alternative stable states, limits cycles, or a combination of both. This article contributes to a growing body of studies about the dynamics of mutualistic–antagonistic communities and hybrid interactions [13,30–34]. The majority of these studies are based on mutualisms such as pollination or seed dispersal, in which the mutualist interacts directly with plants (here prey) but not with herbivores (here predators). In this article the mutualist interacts with both parties of a victim–exploiter pair at the same time.

Our work is relevant for systems in which ants provide defense for plants against their insect herbivores, or defense to herbivores against their insect predators. The first category includes the well known associations such as *Acacia–Pseudomyrmex* [23] and those involving *Macaranga sp.* and symbiont and non-symbiont ants [19] and the plant–ant interaction networks in *cerrado* savannas in Brazil [38]. The second category includes associations of ants with aphids, scale insects, or lepidopteran larvae [49]. Ant-based mutualisms are very relevant for the diversity and stability of plant–animal communities, and for agroecosystems where insect herbivores, such as aphids or scale insects, can turn into pests when protected by ants [12,50,51].

Our model for three species, prey, predator and mutualistic ants, does not consider birth-and-death rates in the case of the mutualist population (unlike e.g., Addicott and Freedman [2], Freedman et al. [10], Rai et al. [40] where birth-vs-death

processes are considered implicitly or explicitly). Instead, ant recruitment is driven by foraging preferences for resources provided by the prey, against competing alternatives, resulting in more or less "visitations" of the prey–predator system by ants. Using analytical and numerical methods, we predict coexistence of predators and prey at alternative equilibria and/or along limit cycles. When ants specialize either on resources provided by the prey/plant or they specialize on the alternative resource, the prey isocline is decreasing with the prey density which leads to local stability of the corresponding equilibria similarly as in the Rosenzweig and MacArthur [45] predator-prey model.

The Rosenzweig–MacArthur model considers handling time predators need to process prey which causes the prey isocline being hump-shaped and leads to emergence of a globally stable limit cycle. In this article we assume that handling time is zero but it is adaptive preference of ants that tracks prey abundance once it passes a critical threshold ($P > \pi_0$) that causes a part of the prey isocline being hump-shaped. Thus, "effective" predation rates display diminishing returns, like in the type II functional response, used in Rosenzweig–MacArthur models. It is also important to stress that in the Rosenzweig–MacArthur model limit cycles result from decelerating predation due to handling time, which allows prey to escape predatory regulation [44,45]. In the current model, limit cycles arise because at high enough prey densities ant recruitment increases and ants interfere with predators which decreases the predation rate. Indeed, without ant recruitment driven by adaptive ant foraging preferences, Eq. (1) would predict global predator-prey stability at an equilibrium.

On contrary to a single stable limit cycle in the Rosenzweig–MacArthur predator-prey model, adaptive ant foraging can lead to multiple locally stable/unstable limit cycles. Here unstable cycles enable scenarios such as *alternative stable cycles* (Fig. 4b), bi-stability (Fig. 4d), or outcomes in which the prey–predator interaction converges to stable coexistence or non-equilibrium coexistence depending on initial conditions (Fig. 4c,e,f). These complex dynamics are more likely when ant interference on predation is strong (large q) and foraging rates or efficiency are low (small b or large w, respectively). The maximum amplitude of prey oscillations tends to increase with ant interference. Thus, strong interference by adaptive mutualistic foragers tends to destabilize prey–predator population dynamics and promotes stronger dependence on initial conditions.

Another interesting feature of the model is the emergence of limit cycles and equilibria at switching boundaries ϕ_0 (11) or ϕ_1 (14) in the $M - F$ parameter space. In one case limit cycles arise at the transition from equilibrium E_0 (where ants specialize on alternative resources) to E_+ (where ants are generalists feeding on both resources), similarly to the super-critical Hopf bifurcation (Fig. 4a). In the other case where E_0 (which is locally stable equilibrium) collides with E_- (which is a saddle point), an unstable cycle emerges (see point **hb** in Fig. 3). This phenomenon corresponds to the situation in which a segment of the predator isocline (8) overlaps with a switching threshold (5) in phase space (Fig. 6). These bifurcations are due to non-smoothness of predator-prey population dynamics (1) with adaptive ant preferences (4). Such continuous but non-smooth dynamical systems are discussed in the book of Simpson [47]. Interestingly, an article by Wu et al. [55] demonstrates the so called *discontinuous Hopf bifurcations* coinciding with harvesting thresholds under spatio-temporal dynamics.

By combining methods of dynamical system analysis and evolutionary game theory, we predict that defensive benefits provided by ants to prey are variable, and depend on feedback between prey–predator population dynamics (1), and behavioral adaptations of ants which can forage on alternative sources (4), like e.g., nectar (honeydew) or another plant (insect prey). This drives the combined demography–behavior dynamics across conditions where prey interfere indirectly with predation through the ants. This is an example of indirect trait-mediated interaction [TMI, 3] where one species (*prey*) affects a second one (*predator*) by altering the behavior of a third species (*ant*). This differs from other kinds of indirect interactions, such as apparent competition [22] or resource competition [16], where two species affect one another by increasing the birth rates of a common predator in the first case, or by depleting their common resource in the second. In our model, the third party (ants) does not experience such demographic changes but changes its foraging preferences. In previous works [28,41–43] we predicted that TMI can lead to alternative stable states for plant–pollinator and mixed mutualistic–antagonistic interactions. In this paper we found that TMI enable even more complex outcomes, such as predator-prey coexistence at alternative non-equilibrium states (e.g., the two coexisting locally stable limit cycles in Fig. 4b) and periodic switching of ants between mutualism and neutralism (e.g., oscillations spanning conditions where ants interact ($0 < u \leq 1$) or do not interact ($u = 0$) with prey, see Fig. 4b–e).

According to our model, ant preferences, and thus predation interference, can be altered by alternative food sources (e.g., other prey, artificial sources). Specifically, increasing such alternative sources weakens defensive ant–prey mutualisms. This prediction finds support in experiments performed by Nagy et al. [36], 37] with ant–aphid–plant systems. The researchers demonstrated that supplementary food such as honey or sucrose solutions can divert ants (*Lassius niger*) from tending aphids (*Dysaphis plantaginea* or *Aphis pomi*), resulting in increased predation by their natural enemies. This illustrates a potential method for improving biological control of insect pests. In this context, our prediction of alternative states, stable and unstable ones, are relevant and worth of experimental investigation. As shown in Figs. 3 and 5, the interplay between prey–predator oscillations and adaptive ant preference extends protection mutualism beyond the point where ants would reject interaction with prey at an equilibrium. However, such extended protection is periodic and can collapse if external perturbations (e.g., an herbicide or pesticide application) are strong enough.

Population dynamics (1) with adaptive mutualism (4) also demonstrate *hysteresis*, e.g., sudden switch from the pest state (e.g., high aphid density) to the controlled state (low aphid density) that depends on the past history of the system (Fig. 3e and f). Similarly, hysteresis also occurs between coexistence along the large amplitude limit cycle and equilibrium E_0 (Fig. 3c–f). Interestingly, hysteresis phenomena are suspected to play an important role for diversity and dynamics of coffee–

ant agroecosystems [50], but this system is much more complex than our model because the focal ant species (*Azteca sp.*) interacts with many plants and insects at the same time.

In developing our models we left out several details in order to achieve a higher generality. Future work can modify our model to consider particular details for specific systems. For example, in the case of ant–plant mutualisms there is evidence of trade-offs relating chemical defense and indirect defense by ants [17–20]. These relationships can be used to relate resource supply rates (s) with intrinsic growth rates (r), in order to model the evolution of plant traits and co-evolution of ant–plant mutualism. There is also the issue of costs associated with ant activity such as interference with insect pollinators. And in the case of ant–aphid mutualisms, the association can bring additional cleaning and dispersal benefits for the aphids [6,24].

5.1. Conclusion

Foraging flexibility of prey-defending ants gives rise to complex prey–predator non-smooth dynamics in which alternative states and multiple limit cycles are possible. Alternative resources can distract ants from foraging on prey resource, weakening the ant–prey mutualism and destabilizing predation dynamics. If ant interference effect on predation is strong enough, dynamical regimes with and we ithout ant defense coexist for a wide range of parameters, but such state is prone to catastrophic collapse if the supply of alternative resources is high enough for ants to abandon the mutualism with the prey entirely.

Acknowledgments

This project has received funding from the European Union's Horizon 2020 research and innovation programme under grant agreement no. 955708, project EvoGamesPlus (Evolutionary games and population dynamics: from theory to applications). We thank three anonymous reviewers for comments and suggestions.

Appendix A. Ant fitness and adaptive preference

Let R and S respectively represent the total amount of resources supplied by the prey and by alternative sources, both foraged at the same specific rate b. If uM ants are foraging on R, and $(1-u)M$ are foraging on S, the average foraging rate by M ants is

$$bR\,uM + bS\,(1-u)M = b(uR + (1-u)S)M.$$

We assume that ant fitness W is directly proportional to average per capita consumption rate

$$W := uR + (1-u)S \tag{A.1}$$

where we neglected the common factor b that does not qualitatively change the results.

Resources R and S obey production and consumption dynamics,

$$\frac{dR}{dt} = sP - wR - ubRM$$
$$\frac{dS}{dt} = F - wS - (1-u)bSM,$$

where w is a common loss rate, s is per capita supply rate of prey resources, and F is the supply rate of the alternative resources. We assume that resource dynamics are fast when compared with prey and predator population dynamics (1) and they are at the equilibrium at the current population densities, i.e.,

$$(R,S) = \left(\frac{sP}{w+buM}, \frac{F}{w+b(1-u)M}\right).$$

Substituting (R,S) in W gives us fitness function (3) in the main text.

Now we calculate evolutionarily stable ant foraging preference. This is a strategy that cannot be invaded by any other mutant strategy [29]. Payoffs U and V (2) are given by the distribution $0 \le u \le 1$ of resident ant foraging preferences and the fitness of a mutant ant playing a different strategy $0 \le \tilde{u} \le 1$ in the resident population is

$$W(\tilde{u},u) = \tilde{u}\underbrace{\left(\frac{sP}{w+buM}\right)}_{U(u)} + (1-\tilde{u})\underbrace{\left(\frac{F}{w+b(1-u)M}\right)}_{V(u)}.$$

We observe that (i) when $P \le \pi_0 = \left(\frac{w}{w+bM}\right)\frac{F}{s}$ then payoff when feeding solely on the alternative food is higher than payoff when feeding on the primary prey resource for any resident distribution, i.e., $V(u) > U(u)$ for all $u \in [0,1]$ and the optimal strategy is $u^* = 0$. Similarly, (ii) when $P \ge \pi_1 = \left(\frac{w+bM}{w}\right)\frac{F}{s}$ then payoff when feeding solely on the primary food is higher than payoff when feeding on the alternative resource for any resident distribution, i.e., $V(u) < U(u)$ for all $u \in [0,1]$, thus

$u^* = 0$. For prey resource densities (iii) between π_0 and π_1, the Nash equilibrium must satisfy $U = V$ [21] which yields $u^* = \frac{sP}{sP+F} + \frac{w(sP-F)}{b(sP+F)M}$. Outcomes (i, ii, iii) combine into Eq. (4) in the main text. Because

$$W(u^*, u) - W(u, u) = \frac{(bM(Fu + Ps(u-1)) + w(F - Ps))^2}{bM(F+Ps)(bM(1-u)+w)(bMu+w)} > 0$$

for every $u \neq u^*$, $0 \leq u \leq 1$, the stability condition in the definition of evolutionary stability [21] holds and u^* is evolutionarily stable.

Appendix B. Predator isoclines

When ants are adaptive foragers, the predator isocline consists of up to three vertical segments depending on parameters as we will show now. By definition, a non-trivial predator isocline is the set of all points in the prey-predator phase plane that satisfy

$$\frac{dH}{Hdt} = \left(\frac{eaP}{1+qu(P)M} - m\right) = 0, \tag{A.2}$$

where u is given in (4). Solving this equation for P we obtain the non-trivial isocline that is defined piece-wise

$$P = \begin{cases} P_0^* & \text{if } P_0^* \leq \pi_0 \\ P_-^* & \text{if } \pi_0 < P_-^* < \pi_1 \\ P_+^* & \text{if } \pi_0 < P_+^* < \pi_1 \\ P_1^* & \text{if } P_1^* \geq \pi_1, \end{cases} \tag{A.3}$$

where

$$\begin{aligned} P_0^* &= \tfrac{m}{ea} \\ P_-^* &= \tfrac{ms(bMq+b+qw)-abeF-\sqrt{(ms(bMq+b+qw)-abeF)^2+4abeFms(b-qw)}}{2beas} \\ P_+^* &= \tfrac{ms(bMq+b+qw)-abeF+\sqrt{(ms(bMq+b+qw)-abeF)^2+4abeFms(b-qw)}}{2beas} \\ P_1^* &= \tfrac{m(1+qM)}{ea}. \end{aligned} \tag{A.4}$$

Fig. A.1 represents these solutions as intersections between the piece-wise function

$$\Pi(P) := \begin{cases} \frac{m}{ea} & P \leq \pi_0 \\ \frac{m(1+qMu(P))}{ea} & \pi_0 < P < \pi_1 \\ \frac{m(1+qM)}{ea} & P \geq \pi_1, \end{cases} \tag{A.5}$$

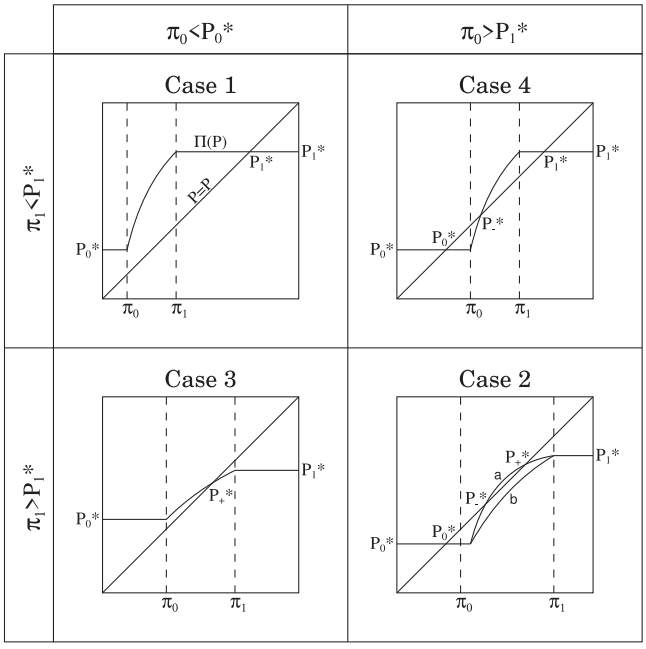

Fig. A.1. Plant equilibria given by intersections of the $\Pi(P)$ function (A.5) and the identity line $P = P$.

and the 45° line. Function $\Pi(P)$ comes from rewriting (A.2) as $P = \frac{m(1+qM\,u(P))}{ea}$ and considering the three cases given in (4). Function $\Pi(P)$ is horizontal for $P \le \pi_0$ and $P \ge \pi_1$, and increasing for $\pi_0 < P < \pi_1$ ($\frac{d\Pi}{dP} > 0$) and concave-down there ($\frac{d^2\Pi}{dP^2} < 0$).

Now we show that the predator isocline consists of one or three vertical segments. We can classify the predator isocline segments by their relative position with respect to thresholds π_0 and π_1 given in (5). We observe that $P_0^* < \pi_0$ iff $F > \frac{ms(bM+w)}{aew} := \phi_0$ and $P_1^* > \pi_1$ iff $F < \frac{msw(1+Mq)}{ae(bM+w)} := \phi_1$. The first condition holds when the alternative resource input rate is relatively high when compared to the prey resource while the second condition requires just the opposite.

We get the following qualitative cases, sketched in Fig. A.1:

1. $\pi_0 < P_0^*$ and $\pi_1 < P_1^*$, i.e., $F < \min\{\phi_0, \phi_1\}$. After some algebra we get that neither $\pi_0 < P_-^* < \pi_1$, nor $\pi_0 < P_+^* < \pi_1$ and the predator isocline consists of a single segment $P = P_1^*$ (see "Case 1" in Fig. A.1).
2. $\pi_0 > P_0^*$ and $\pi_1 > P_1^*$, i.e., $F > \max\{\phi_0, \phi_1\}$. After some algebra we get that $P = P_0^*$ is always a segment of the predator isocline, and there are two possibilities:
   a) there are two additional segments $P = P_-^*$ and $P = P_+^*$ (see curve "a" of "Case 2" in Fig. A.1)[2].
   b) there are no more isocline segments (see curve "b" in "Case 2" in Fig. A.1).
3. $\pi_0 < P_0^*$ and $\pi_1 > P_1^*$, i.e., $\phi_1 < F < \phi_0$. After some algebra we observe that $\pi_0 < P_+^* < \pi_1$ and the predator isocline consists of a single segment $P = P_+^*$ (see "Case 3" in Fig. A.1).
4. $\pi_0 > P_0^*$ and $\pi_1 < P_1^*$, i.e., $\phi_0 < F < \phi_1$. After some algebra we observe that $\pi_0 < P_-^* < \pi_1$ and the predator isocline consists of three segments $P = P_0^*$, $P = P_-^*$,$P = P_1^*$ (see "Case 4" in Fig. A.1).

Appendix C. Stability of equilibria of system (1)

Consider system (1). The prey isocline is the curve

$$\Gamma(P) := \frac{r(K-P)(1+qM\,u(P))}{aK}. \tag{A.6}$$

in the first quadrant of the phase plane. Because ant foraging strategy u given in (4) is defined piece-wised, $\Gamma(P)$ is also defined piece-wise. We observe that $\Gamma(P)$ is continuous and for $P \notin \{\pi_0, \pi_1\}$

$$\frac{d\Gamma}{dP} = \frac{qM\Gamma(P)}{1+qu(P)M}\left\{\frac{du}{dP} - \frac{r(1+qu(P)M)^2}{aqMK\Gamma(P)}\right\}, \tag{A.7}$$

where π_0 and π_1 are given in (5).

The predator isocline consists of vertical segments $P = P_i^* > 0$ $(i = 1, 2, 3)$ in the phase space, where P_i^* satisfies equation $P = \Pi(P)$ (Appendix B, Fig. A.1). The curve (A.5) has a derivative for $P \notin \{\pi_0, \pi_1\}$

$$\frac{d\Pi}{dP} = \frac{mqM}{ea}\frac{du}{dP}. \tag{A.8}$$

A coexistence equilibrium is a point $E_i = (P_i^*, H_i^*)$ where $H_i^* = \Gamma(P_i^*) > 0$. The Jacobian matrix of system (1) evaluated at E_i is

$$\begin{bmatrix} \frac{\partial \dot P}{\partial P} & \frac{\partial \dot P}{\partial H} \\ \frac{\partial \dot H}{\partial P} & \frac{\partial \dot H}{\partial H} \end{bmatrix}_{E_i} = \begin{bmatrix} P\left(\frac{aqHM}{(1+qu(P)M)^2}\frac{du}{dP} - \frac{r}{K}\right) & -\frac{aP}{1+qu(P)M} \\ \frac{eaqMPH}{(1+qu(P)M)^2}\left(\frac{1+qu(P)M}{qMP} - \frac{du}{dP}\right) & 0 \end{bmatrix}_{(P_i^*, H_i^*)}.$$

Equilibrium E_i is locally asymptotically stable if the trace and determinant of the Jacobian matrix

$$T_i = \left(\frac{\partial \dot P}{\partial P} + \frac{\partial \dot H}{\partial H}\right)\Big|_{E_i} = P\left(\frac{aqMH_i^*}{(1+qu(P_i^*)M)^2}\frac{du}{dP}\Big|_{P_i^*} - \frac{r}{K}\right)$$

$$\Delta_i = \left(\frac{\partial \dot P}{\partial P}\frac{\partial \dot H}{\partial H} - \frac{\partial \dot P}{\partial H}\frac{\partial \dot H}{\partial P}\right)\Big|_{E_i} = \frac{ea^2qMP_i^{*2}H_i^*}{(1+qu(P_i^*)M)^3}\left(\frac{1+qu(P_i^*)M}{qMP_i^*} - \frac{du}{dP}\Big|_{P_i^*}\right),$$

are negative ($T_i < 0$) and positive ($\Delta_i > 0$), respectively. Since $\Gamma(P_i^*) = H_i^*$, and substituting du/dP from (A.7) we get

$$T_i = \frac{aP_i^*}{1+qu(P_i^*)M}\frac{d\Gamma}{dP}\Big|_{P_i^*}.$$

[2] We disregard the non-generic case where $P_-^* = P_+^*$ (i.e., the $\Pi(P)$ curve is tangent to the 45° line)

We use (A.5) and (A.8) to replace $1+qMu$ by $\frac{ea\Pi}{m}$ and $\frac{\partial u}{\partial P}$ by $\frac{ea}{mqM}\frac{d\Pi}{dP}$ in the expression for the determinant which yields

$$\Delta_i := \frac{e^2a^3P_i^{*2}H_i^*}{m(1+qu(P_i^*)M)^3}\left(\frac{\Pi(P_i^*)}{P_i^*}-\left.\frac{d\Pi}{dP}\right|_{P_i^*}\right)=\frac{e^2a^3P_i^{*2}H_i^*}{m(1+qu(P_i^*)M)^3}\left(1-\left.\frac{d\Pi}{dP}\right|_{P_i^*}\right),$$

where $P_i^*=\Pi(P_i^*)$ at a non-trivial equilibrium.

Next, we use Fig. 2 from the main text and Fig. A.1 from Appendix B, to determine stability of equilibrium points E_0, E_-, E_+, E_1 corresponding to $P_0^*, P_-^*, P_+^*, P_1^*$ from Appendix B:

- E_0 is locally asymptotically stable because $\left.\frac{d\Pi}{dP}\right|_{P_0^*}=0$ (Fig. A.1 panels II, IV) implies $\Delta_0>0$ and since $\left.\frac{d\Gamma}{dP}\right|_{P_0^*}<0$ (decreasing prey isocline, e.g., see Fig. 2b,c,e) implies $T_0<0$.
- E_1 is locally stable because $\left.\frac{d\Pi}{dP}\right|_{P_1^*}=0$ (Fig. A.1 panels I, IV) implies $\Delta_1>0$ and since $\left.\frac{d\Gamma}{dP}\right|_{P_1^*}<0$ (decreasing prey isocline, e.g., see Fig. 2a and e) implies $T_1<0$.
- E_- is locally unstable because $\left.\frac{d\Pi}{dP}\right|_{P_-^*}>0$ (Fig. A.1 panels II.a, IV) implies $\Delta_-<0$. The eigenvalues of E_- are $\frac{T_-\pm\sqrt{T_-^2-4\Delta_-}}{2}$, i.e., real and with different signs, i.e., E_- is a saddle.
- E_+ can be either locally stable or unstable. Because $\left.\frac{d\Pi}{dP}\right|_{P_+^*}<0$, $\Delta_+>0$ (Fig. A.1 panels II.a, III). Thus, this equilibrium is
  - locally asymptotically stable if $\left.\frac{d\Gamma}{dP}\right|_{P_+^*}<0$ (decreasing prey isocline, e.g., Fig. 2b) which makes $T_+<0$.
  - unstable if $\left.\frac{d\Gamma}{dP}\right|_{P_+^*}>0$ (increasing prey isocline, e.g., Fig. 2d) which makes $T_+>0$.

Appendix D. Note about numerical bifurcation

Curves **SN** (18), **HB, fc**, and **FC** in Fig. 5 were obtained using XPPAUT [8]. Saddle–node curves (**SN**) and Hopf bifurcations (**HB**) can be continued accurately in the $M-F$ plane. To continue fold bifurcations of limit cycles (**fc** and **FC**) we used a smooth version of the piece-wise defined function u given in (4)

$$u(P)=\mathrm{smax}\left(0,\ \mathrm{smin}\left(1,\ \frac{sP}{sP+F}+\frac{w(sP-F)}{b(sP+F)M}\right)\right),$$

where

$$\mathrm{smax}(x,y)=\frac{xe^{\alpha x}+ye^{\alpha y}}{e^{\alpha x}+e^{\alpha y}},\ \mathrm{smin}(x,y)=\frac{xe^{-\alpha x}+ye^{-\alpha y}}{e^{-\alpha x}+e^{-\alpha y}},$$

are smooth approximations of maximum and minimum functions, respectively. Here e is the base of natural logarithms, and the approximation of (4) improves as exponent α increases. In our numerical simulations we used $\alpha=100$ which gives a very good approximation.

References

[1] P.A. Abrams, R. Cressman, V. Křivan, Role of behavioral dynamics in determining the patch distributions of interacting species, Am. Nat. 169 (4) (2007) 505–518, doi:10.1086/511963.
[2] J.F. Addicott, H.I. Freedman, On the structure and stability of mutualistic systems: analysis of predator-prey and competition models as modified by the action of a slow-growing mutualist, Theor. Popul. Biol. 26 (3) (1984) 320–339, doi:10.1016/0040-5809(84)90037-6.
[3] B. Bolker, M. Holyoak, V. Křivan, L. Rowe, O. Schmitz, Connecting theoretical and empirical studies of trait-mediated interactions, Ecology 84 (5) (2003) 1101–1114, doi:10.1890/0012-9658(2003)084[1101:CTAESO]2.0.CO;2.
[4] T. Case, An Illustrated Guide to Theoretical Ecology, Oxford University Press, 2000.
[5] R. Colombo, V. Křivan, Selective strategies in food webs, IMA J. Math. Appl. Med. Biol. 10 (1993) 281–291.
[6] R. Durak, E. Węgrzyn, K. Leniowski, When a little means a lot–slight daily cleaning is crucial for obligatory ant-tended aphids, Ethol. Ecol. Evol. 28 (1) (2016) 20–29, doi:10.1080/03949370.2014.952340.
[7] L. Elizalde, M. Arbetman, X. Arnan, P. Eggleton, I.R. Leal, M.N. Lescano, A. Saez, V. Werenkraut, G.I. Pirk, The ecosystem services provided by social insects: traits, management tools and knowledge gaps, Biol. Rev. 95 (5) (2020) 1418–1441, doi:10.1111/brv.12616.
[8] B. Ermentrout, Simulating, Analyzing, and Animating Dynamical Systems: a Guide to XPPAUT for Researchers and Students, first ed., Society for Industrial and Applied Mathematics, Philadelphia, 2002.
[9] A.F. Filippov, Differential Equations with Discontinuous Righthand Sides, Kluwer Academic Publishers, 1988.
[10] H. Freedman, J.F. Addicott, B. Rai, Obligate mutualism with a predator: stability and persistence of three-species models, Theor. Popul. Biol. 32 (2) (1987) 157–175, doi:10.1016/0040-5809(87)90045-1.
[11] S.D. Fretwell, H.L. Lucas, On territorial behavior and other factors influencing habitat distribution in birds. I. Theoretical development, Acta Biotheor. 19 (1969) 16–36, doi:10.1007/BF01601953.
[12] L. Garcia-Barrios, I. Perfecto, J. Vandermeer, Azteca chess: gamifying a complex ecological process of autonomous pest control in shade coffee, Agric. Ecosyst. Environ. 232 (2016) 190–198, doi:10.1016/j.agee.2016.08.014.
[13] E. Georgelin, N. Loeuille, Dynamics of coupled mutualistic and antagonistic interactions, and their implications for ecosystem management, J. Theor. Biol. 346 (7) (2014) 67–74, doi:10.1016/j.jtbi.2013.12.012.
[14] A.J. Golubski, P.A. Abrams, Modifying modifiers: what happens when interspecific interactions interact? J. Anim. Ecol. 80 (5) (2011) 1097–1108, doi:10.1111/j.1365-2656.2011.01852.x.
[15] J. Gómez, R. Zamora, Pollination by ants: consequences of the quantitative effects on a mutualistic system, Oecologia 91 (3) (1992) 410–418, doi:10.1007/BF00317631.
[16] J.P. Grover, Resource Competition, Population and Community Biology Series, Chapman & Hall, London, 1997.

[17] M. Heil, Indirect defence via tritrophic interactions, New Phytol. 178 (1) (2008) 41–61, doi:10.1111/j.1469-8137.2007.02330.x.
[18] M. Heil, B. Fiala, K.E. Linsenmair, G. Zotz, P. Menke, Food body production in *Macaranga triloba*(Euphorbiaceae): a plant investment in anti-herbivore defence via symbiotic ant partners, J. Ecol. 85 (6) (1997) 847–861, doi:10.2307/2960606.
[19] M. Heil, B. Fiala, U. Maschwitz, K.E. Linsenmair, On benefits of indirect defence: short-and long-term studies of antiherbivore protection via mutualistic ants, Oecologia 126 (3) (2001) 395–403, doi:10.1007/s004420000532.
[20] M. Heil, C. Staehelin, D. McKey, Low chitinase activity in acacia myrmecophytes: a potential trade-off between biotic and chemical defences? Naturwissenschaften 87 (12) (2000) 555–558, doi:10.1007/s001140050778.
[21] J. Hofbauer, K. Sigmund, Evolutionary Games and Population Dynamics, Cambridge University Press, 1998.
[22] R.D. Holt, Predation, apparent competition, and the structure of prey communities, Theor. Popul. Biol. 12 (1977) 197–229, doi:10.1016/0040-5809(77)90042-9.
[23] D.H. Janzen, Coevolution of mutualism between ants and acacias in central America, Evolution 20 (3) (1966) 249–275, doi:10.2307/2406628.
[24] S. Jha, D. Allen, H. Liere, I. Perfecto, J. Vandermeer, Mutualisms and population regulation: mechanism matters, PLoS One 7 (8) (2012) e43510, doi:10.1371/journal.pone.0043510.
[25] V. Křivan, Dynamic ideal free distribution: effects of optimal patch choice on predator-prey dynamics, Am. Nat. 149 (1) (1997) 164–178, doi:10.1086/285984.
[26] V. Křivan, Prey-predator models, in: S.E. Jørgensen, B.D. Fath (Eds.), Prey–Predator Models, vol. 5, Elsevier, 2008, pp. 2929–2940.
[27] V. Křivan, R. Cressman, C. Schneider, The ideal free distribution: a review and synthesis of the game-theoretic perspective, Theor. Popul. Biol. 73 (2008) 403–425, doi:10.1016/j.tpb.2007.12.009.
[28] V. Křivan, T.A. Revilla, Plant coexistence mediated by adaptive foraging preferences of exploiters or mutualists, J. Theor. Biol. 480 (2019) 112–128, doi:10.1016/j.jtbi.2019.08.003.
[29] J. Maynard Smith, G.R. Price, The logic of animal conflict, Nature 246 (5427) (1973) 15–18, doi:10.1038/246015a0.
[30] C.J. Melián, J. Bascompte, P. Jordano, V. Křivan, Diversity in a complex ecological network with two interaction types, Oikos 118 (1) (2009) 122–130, doi:10.1111/j.1600-0706.2008.16751.x.
[31] A. Mougi, M. Kondoh, Diversity of interaction types and ecological community stability, Science 337 (6092) (2012) 349–351, doi:10.1126/science.1220529.
[32] A. Mougi, M. Kondoh, Adaptation in a hybrid world with multiple interaction types: a new mechanism for species coexistence, Ecol. Res. 29 (2) (2014) 113–119, doi:10.1007/s11284-013-1111-4.
[33] A. Mougi, M. Kondoh, Instability of a hybrid module of antagonistic and mutualistic interactions, Popul. Ecol. 56 (2) (2014) 257–263, doi:10.1007/s10144-014-0430-9.
[34] A. Mougi, M. Kondoh, Stability of competition–antagonism–mutualism hybrid community and the role of community network structure, J. Theor. Biol. 360 (2014) 54–58, doi:10.1016/j.jtbi.2014.06.030.
[35] J.D. Murray, Mathematical Biology I: an Introduction, Interdisciplinary Applied Mathematics, vol. 17, 3rd ed., Springer, 2002.
[36] C. Nagy, J.V. Cross, V. Markó, Sugar feeding of the common black ant, *Lasius niger* (L.), as a possible indirect method for reducing aphid populations on apple by disturbing ant-aphid mutualism, Biol. Control 65 (1) (2013) 24–36, doi:10.1016/j.biocontrol.2013.01.005.
[37] C. Nagy, J.V. Cross, V. Markó, Can artificial nectaries outcompete aphids in ant-aphid mutualism? Applying artificial sugar sources for ants to support better biological control of rosy apple aphid, dysaphis plantaginea passerini in apple orchards, Crop Prot. 77 (2015) 127–138, doi:10.1016/j.cropro.2015.07.015.
[38] P.S. Oliveira, A.V. Freitas, Ant–plant–herbivore interactions in the neotropical cerrado savanna, Naturwissenschaften 91 (12) (2004) 557–570, doi:10.1007/s00114-004-0585-x.
[39] G. Parker, Searching for mates, in: Behavioural Ecology: an Evolutionary Approach, Blackwell, Oxford, 1978, pp. 214–244.
[40] B. Rai, H.I. Freedman, J.F. Addicott, Analysis of three species models of mutualism in predator-prey and competitive systems, Math. Biosci. 65 (1) (1983) 13–50, doi:10.1016/0025-5564(83)90069-X.
[41] T.A. Revilla, V. Křivan, Pollinator foraging adaptation and the coexistence of competing plants, PLoS One 11 (8) (2016) e0160076, doi:10.1371/journal.pone.0160076.
[42] T.A. Revilla, V. Křivan, Competition, trait-mediated facilitation, and the structure of plant-pollinator communities, J. Theor. Biol. 440 (2018) 42–57, doi:10.1016/j.jtbi.2017.12.019.
[43] T.A. Revilla, T. Marcou, V. Křivan, Plant competition under simultaneous adaptation by herbivores and pollinators, Ecol. Model. 455 (2021) 109634, doi:10.1016/j.ecolmodel.2021.109634.
[44] M.L. Rosenzweig, Why the prey curve has a hump, Am. Nat. 103 (929) (1969) 81–87. http://www.jstor.org/stable/10.2307/2459470.
[45] M.L. Rosenzweig, R.H. MacArthur, Graphical representation and stability conditions of predator-prey interactions, Am. Nat. 97 (1963) 209–223. http://www.jstor.org/stable/2458702.
[46] O.J. Schmitz, V. Křivan, O. Ovadia, Trophic cascades: the primacy of trait-mediated indirect interactions, Ecol. Lett. 7 (2) (2004) 153–163, doi:10.1111/j.1461-0248.2003.00560.x.
[47] D. Simpson, Bifurcations in Piecewise-Smooth Continuous Systems, World Scientific Series on Nonlinear Science Series a, WS, 2010. http://gen.lib.rus.ec/book/index.php?md5=d1d926aee729cbcecb87a98cdf3eb7aa.
[48] B. Stadler, A.F. Dixon, Ecology and evolution of aphid-ant interactions, Annu. Rev. Ecol., Evol. Syst. 36 (2005) 345–372, doi:10.1146/annurev.ecolsys.36.091704.175531.
[49] B. Stadler, A.F.G. Dixon, Mutualism: Ants and their Insect Partners, first ed., Cambridge University Press, 2008. http://gen.lib.rus.ec/book/index.php?md5=16035C63745947CC3B5818B324490EFB.
[50] J. Vandermeer, I. Perfecto, Hysteresis and critical transitions in a coffee agroecosystem, Proc. Natl. Acad. Sci. U. S. A. 116 (30) (2019) 15074–15079, doi:10.1073/pnas.1902773116.
[51] J. Vandermeer, I. Perfecto, S. Philpott, Ecological complexity and pest control in organic coffee production: uncovering an autonomous ecosystem service, Bioscience 60 (7) (2010) 527–537, doi:10.1525/bio.2010.60.7.8.
[52] W. Völkl, J. Woodring, M. Fischer, M.W. Lorenz, K.H. Hoffmann, Ant-aphid mutualisms: the impact of honeydew production and honeydew sugar composition on ant preferences, Oecologia 118 (4) (1999) 483–491, doi:10.1007/s004420050751.
[53] D. Wagner, A. Kay, Do extrafloral nectaries distract ants from visiting flowers? An experimental test of an overlooked hypothesis, Evol. Ecol. Res. 4 (2) (2002) 293–305.
[54] N.A. Weber, Fungus-growing ants, Science 153 (3736) (1966) 587–604, doi:10.1126/science.153.3736.587.
[55] D. Wu, H. Zhao, Y. Yuan, Complex dynamics of a diffusive predator–prey model with strong Allee effect and threshold harvesting, J. Math. Anal. Appl. 469 (2) (2019) 982–1014, doi:10.1016/j.jmaa.2018.09.047.
[56] X. Zhang, H. Zhao, Dynamics analysis of a delayed reaction-diffusion predator-prey system with non-continuous threshold harvesting, Math. Biosci. 289 (2017) 130–141, doi:10.1016/j.mbs.2017.05.007.